Hoang. *Journal of Southern Hemisphere Earth Systems Science* (2016) 66:424–441. DOI: 10.22499/3.6604.004

Coherent Potential Vorticity Maxima and Their Relationship to Extreme Summer Rainfall in the Australian and North African Tropics

Lam P. Hoang,[1,2,3], Michael J. Reeder[2,3], Gareth. J. Berry[4] and Juliane Schwendike[4]

[1] Vietnam National Centre for Hydro-Meteorological Forecasting, Hanoi, Vietnam
[2] School of Earth, Atmosphere and Environment, Monash University, Clayton, Victoria, Australia
[3] ARC Centre of Excellence for Climate System Science, Monash University, Clayton, Victoria, Australia
[4] Institute for Climate and Atmospheric Science, School of Earth and Environment, University of Leeds, UK

(Manuscript received April 2016; accepted November 2016)

Extreme rainfall in the tropics is frequently linked with coherent synoptic-scale potential vorticity (PV) disturbances. Here, an objective technique is used to identify coherent synoptic-scale cyclonic PV maxima with a focus on those that occur during summer over the African and Australian tropics. These two regions are chosen for comparison because of their geographical and climatological similarities. In particular, in both regions oceans lie equatorward and extensive deserts lie poleward, a juxtaposition that produces a reversal in the mean north-south temperature gradient and, through thermal wind, a low level easterly jet.

In general, in the lower troposphere there are more coherent PV maxima in the tropics in the summer hemisphere than the winter hemisphere. These coherent PV maxima generally move with the background flow in the lower troposphere. The largest meridional flux of coherent PV maxima lies along eastern Australia with about half of the coherent PV maxima generated through the filamentaton and eventual isolation of midlatitude PV. In contrast, in the north African tropics, coherent PV maxima are generated mostly in the tropics and move westward through the west African monsoon region.

Composites based on the extreme rainfall days for two regions are broadly similar with large, statistically significant PV maxima to the east of the maximum positive rainfall anomalies. The vertical structures of the PV fields in the two regions reveal a cyclonic PV maximum in the mid-troposphere collocated with the maximum of diabatic heating. The composite horizontal wind structures in the Australian tropics show structures similar to mesoscale convective systems (MCSs), whereas in the African tropics, they are similar to easterly waves.

Corresponding author: Lam P. Hoang, National Centre for Hydro-Meteorological Forecasting, No 8, Phao Dai Lang street, Dong Da district Hanoi, Vietnam
Email: lam.hoang@monash.edu

1. Introduction

Synoptic-scale weather systems in the tropics are often associated with pronounced cyclonic vorticity anomalies in the lower and middle troposphere. African Easterly Waves over tropical north Africa are a particularly well-known and well-studied example (e.g. Carlson 1969, Reed et al. 1977, Pytharoulis and Thorncroft 1999, Berry and Thorncroft 2005, Berry and Thorncroft 2011). Other well-known examples include monsoon lows in the Bay of Bengal (e.g. Godbole 1977) and monsoon depressions in the Australian region (e.g. Davidson and Holland 1987, Mills and Zhao 1991, Hell and Smith 1998, Kong and Zhao 2010).

The geographical and climatological similarities between tropical north Africa and tropical northern Australia prompted Dickinson and Molinari (2000) to ask whether or not the same dynamical processes were relevant in the two regions, which was evaluated by examining changes in the sign of the meridional PV gradient. These authors found that, like north Africa, the Australian tropics are characterized by an easterly jet in which the meridional PV gradient changes sign, although the length of the region in which the gradient is reversed is around 3000 km compared with 5000 km over north Africa. Using spectral methods, they concluded, however, that there was no evidence for African Easterly Wave-like disturbances over northern Australia.

Recently, the climatological structure and evolution of synoptic-scale weather systems in the Australian tropics have been examined by Berry et al. (2012) by tracking isolated cyclonic PV maxima, termed by the authors coherent PV anomalies. Their results challenge the conclusions of Dickinson and Molinari (2000) as it was found that these coherent PV maxima resemble African Easterly Waves. Although most of these coherent PV maxima develop within the Australian monsoon, around a third are first detected in the sub-tropics or extratropics, particularly near the eastern coast of the Australian continent. The time interval between successive coherent PV maxima is highly variable with a mean of about 2.5 days. However, the rainfall in the Australian tropics is often coincident with the passage of these coherent PV maxima, and in some parts of northwestern Australia, the associated rainfall accounts for up to half the annual rainfall (Berry et al. 2012).

Building on the work of Berry et al. (2012), the first aim of the present study is to establish the relationship between extreme rainfall in the Australian tropics and coherent cyclonic PV maxima. The work will answer the questions: What is the PV structure of extreme rain events and are these structures coherent cyclonic PV maxima? The second aim of the present study is to assess the extent to which the PV dynamics of extreme rainfall in the Australian and north African tropics are similar. Specifically the paper will answer the question: What are the similarities and differences between the PV structures responsible for extreme rain events in the Australian and north African tropics?

The remainder of the paper is structured as follows. The data and research methods are discussed in Section 2. This is followed by a description of the climatology of coherent cyclonic PV maxima and extreme rainfall in Section 3. Section 4 examines the composite synoptic structure of the extreme rainfall-producing systems in the Australian tropics. Section 5 applies a similar analysis to tropical north Africa. The conclusions and discussion are presented in Section 6.

2. Data and Methods

The two principal data sets used here are the European Centre for Medium-Range Weather Forecasts (ECMWF) ERA-Interim reanalysis (Simmons et al. 2007) and the Global Precipitation Climate Project (GPCP) 1-Degree Daily Combination (version 1.2) (Huffman et al. 2001). The ERA-Interim data used here span the period from 1980 to 2009, every six hours with a horizontal resolution of 1.5 degrees. Throughout the paper, PV in the Southern Hemisphere is multiplied by negative one (-1) so that positive values and their maxima are cyclonic in both hemispheres.

A coherent PV maximum is defined as a local maximum of at least 0.1 PV unit (PVU, 1 PVU = 10^{-6} K m^2 kg^{-1} s^{-1}) within a radius of six degrees. Those coherent maxima from consecutive time steps which are sufficiently close are joined to form a track. Determining the track comprises two steps. First, the locations of existing PV maxima six hours later are predicted using the isentropic winds interpolated to the location of the PV maxima. Second, if the coherent PV maxima identified in the next time step are within five degrees of a forecast position they are assumed to be the same maximum and are joined to form a track. Coherent PV maxima are tracked on three isentropic surfaces (315 K, 330 K and 350 K, which are approximately 700 hPa, 500 hPa and 200 hPa). After constructing the tracks for all coherent PV maxima, a climatology is calculated for those maxima with lifetimes of at least two days.

Berry et al. (2012) investigated the origin of the coherent PV maxima in the Australian tropics and concluded that some originated in the extratropics. In the extratropics, however, PV maxima are often filamented while still remaining attached to the high-latitude PV reservoir (i.e. these PV maxima correspond to extratropical troughs). As the PV maxima are not isolated, the algorithm is unable to track them. To investigate whether or not the coherent PV maxima originate in the extratropics, three-dimensional air parcel 5-day back trajectories are computed from the first detected point using the wind components from the 6-hourly ERA-Interim reanalysis. Trajectories are calculated for all the parcels within a box of 10 $\times$ 10 degrees centred at the first detected positions on the pressure level nearest the respective isentropic surface (i.e. 700, 500 and 200 hPa for maxima located on the 315, 330 and 350 K surfaces, respectively) .

The diabatic heating rate is derived from ERA-Interim data and is calculated as the residual from the diabatic heating budget according to the expression

$$\dot{H} = -\pi c_p \left(\frac{\partial \theta}{\partial t} + u\frac{\partial \theta}{\partial x} + v\frac{\partial \theta}{\partial y} + \omega\frac{\partial \theta}{\partial p} \right) \tag{1}$$

where θ is the potential temperature, $\dot{H}$ is the diabatic heating rate per unit mass, u and v are the zonal and meridional components of the velocity and ω is the vertical motion in pressure coordinates. $\pi = (p/p_0)^{R/c_p}$ is the Exner function where p_0 is the reference pressure of 1000 hPa, p is the pressure, R is the gas constant for dry air, and c_p is heat capacity of dry air at constant pressure.

Berry and Reeder (2013) introduced a method to objectively identify the ITCZ in gridded data sets. In their study, the ITCZ is defined as a line of convergence along which the magnitude of horizontal gradient of divergence is equal to zero (see Berry and Reeder 2013 for details). In the present study their method is used to determine the position of the ITCZ in the ERA-Interim reanalysis, although the feature identified by this method is termed the monsoon trough.

The GPCP data are used to identify extreme rain days. Extreme rainfall in a region for a particular season is defined by the 95th percentile of the area-averaged daily rainfall from 1997 to 2009. This time interval is also used to calculate the climatological daily mean and the daily rainfall anomaly therefrom.

Much of the analysis focuses on two compositing regions, one in the Australian tropics and one in the north African tropics. The Australian composite region is located west of Darwin and is defined by the box 10-20°S, 125-130°E. This box is chosen for consistency as it the same as that used by Berry et al. (2012). It was chosen by these authors as it covered the maximum in the number of summertime coherent PV maxima on the 330 K surface. The north African composite region lies in the west of Nigeria and is defined by the box 5–15°N, 0–5°E (red boxes in Fig. 1). It was chosen because it lies in a region in which the number of coherent PV maxima is a maximum. The results for both the Australian and north African regions are not sensitive to changes in the position of the box, provided they are located on the strip along which the flux of coherent PV maxima is large (see the next section).

In this research, the composite values at each grid point will be compared to the random sample of 10000 members generated by the bootstrap resampling with replacement approach (see Efron and Tibshirani 1993). Each member of the random sample is the mean value of n random days, where n is number of extreme rainfall days in the respective season and region (60 days in DJF for the Australian tropics and 61 days in JJA for the north African tropics). The composite value is considered significant if it is greater than 95 per cent of the values in the random sample (i.e. it has a p-value less than 0.05). Although significance testing is commonly used, its value and appropriateness has been questioned by Gill (1999), Johnson (1999) and Nicholls (2001) among others.

3. Climatology of Potential Vorticity Maxima and Extreme Rainfall

3.1 Global Climatology of Potential Vorticity Maxima

A climatology of the number of coherent PV maxima on the 315 K surface in December, January, and February (DJF) and June, July, and August (JJA) along with their mean motion vectors (derived from the mean of the individual tracks) are shown for the global tropics and subtropics in Fig. 1. Only those areas are plotted in which the number exceeds 60 PV maxima in 30 years (1980–2009). This figure shows that there are more coherent PV maxima in the summer hemisphere than in the winter

hemisphere, and that in the winter hemisphere the coherent PV maxima lie predominantly on the equatorward flank of the subtropical anticyclones. The tracking technique finds few coherent PV maxima at high latitudes where the PV maxima are more commonly part of elongated PV troughs rather than isolated maxima (Berry et al. 2012); the extratropical origin of some coherent PV maxima is investigated using back trajectories in following subsection. Although not shown here, coherent PV maxima on the 330 K and 350 K isentropic surfaces show the same broad seasonal and latitudinal distributions. The regions in which the number of coherent PV maxima exceeds 75 in JJA (Fig. 1b) extend further poleward in the Northern Hemisphere than those in the Southern Hemisphere during DJF (Fig 1a). The highest numbers of coherent PV maxima occur over the eastern Pacific and north-eastern Atlantic in JJA and the western Pacific and north-western Atlantic in DJF. The northern Indian Ocean is one of the few tropical regions where the number of coherent PV maxima is higher in DJF than JJA.

The motion vectors plotted in Fig. 1 show that the 315 K coherent PV maxima commonly circulate around the periphery of the mean subtropical anticyclones. The motion vectors imply the transport of coherent PV maxima from the tropics to the midlatitudes on the western side of the subtropical anticyclones and from the midlatitudes to the tropics on the eastern side. The area in which the meridional transport is largest is the east coast of Australia during DJF where the tracks of the coherent PV maxima curve anticyclonically near 150–160°E, transporting cyclonic PV from the subtropics toward the tropics. These coherent PV maxima then move westward in tropical region with a speed of 2–3 m s^{-1}. On the other hand, over tropical northern Africa, the motion of the PV maxima is mostly zonal, transporting cyclonic PV westward along the tropics with a mean speed of 5–6 m s^{-1}. This difference in direction suggests that some coherent PV maxima in the Australian tropics may originate in the extratropics, whereas over northern Africa, the coherent PV maxima are most commonly generated at low latitudes. The coherent PV maxima in the Australian region on the 330 K isentropic surface also move anticyclonically towards the tropics near 140°E (not shown). However, the region of equatorward transport on the 330 K isentropic surface is both smaller and displaced more equatorward.

Comparing Fig. 1 with previous work by Laing and Fritsch (1997) (especially their Fig. 3b) shows that those areas in which the number of coherent PV maxima are high closely matches regions in which the frequency of mesoscale convective complexes are high also, especially in the tropical land masses of northern Africa in JJA, northern Australia and southern Africa in DJF, and the Maritime Continent. This matching suggests a relationship between coherent PV maxima and mesoscale convective systems (MCSs) in these areas. Moreover, the objective tracking technique used here identifies a large number of coherent PV maxima over the oceans.

3.2 Statistics of Coherent PV Maxima and Parcels Back Trajectories

The mean motion vectors in DJF and JJA (Fig. 1a and b) show, among other things, a meridional transport of extratropical coherent PV maxima toward the tropics over eastern Australia and a zonal transport over the north African tropics. Using these tracks, the genesis positions of the coherent PV maxima crossing the compositing box in the Australian and north African tropics are determined. Defining the extratropics as latitudes poleward of 23.5°, 6.1 per cent, 11.7 per cent and 5.8 per cent of the tracked systems on the 315, 330 and 350 K isentropes respectively that cross the compositing region are first detected in the extratropics. The same calculations for the north African tropics show that none of the coherent PV maxima on the 315 and 350 K isentropes that cross the compositing box are detected first in the extratropics. For those coherent PV maxima on the 330 K isentropes crossing the compositing box, about 3.6 per cent of them are first detected in the extratropics.

It is probable that some of these features are generated in the extratropics, but not detected at higher latitudes due to the limitations of the tracking algorithm; in particular, the algorithm only tracks PV features that have closed contours and is unable to track filaments. For this reason, the source of the air near the centre of a coherent PV maximum within the analysis boxes shown in Fig. 1 is determined using three-dimensional back trajectories from a 10×10 degree grid centreed on the first detected position of the coherent PV maximum. The fraction of air with extratropical origin on the 10×10 degrees grid during the previous 5 days is diagnosed. Table 1 presents the overall statistics of the analysis for the two regions.

In tropical Australia, the proportion of air parcels ending up at 700 hPa, 500 hPa and 200 hPa at the first detected point that comes from maximum latitudes poleward of 23.5°S are 49.4 per cent, 51.3 per cent and 38.4 per cent respectively. The statistics above indicate that about 50 per cent of the low- and middle-level coherent PV maxima in the Australian tropics are associated with air that has recently resided in the extratropics. In the north African tropics, the corresponding proportions are 25.3 per cent, 34.6 per cent and 6.3 per cent. Hence, coherent PV maxima in the Australian tropics are more likely to be associated with extratropical air than their counterparts in the north African tropics. These results suggest that there is a greater link between the tropics and extratropics in the Australian region than in the north African region despite their geographical and climatological similarities.

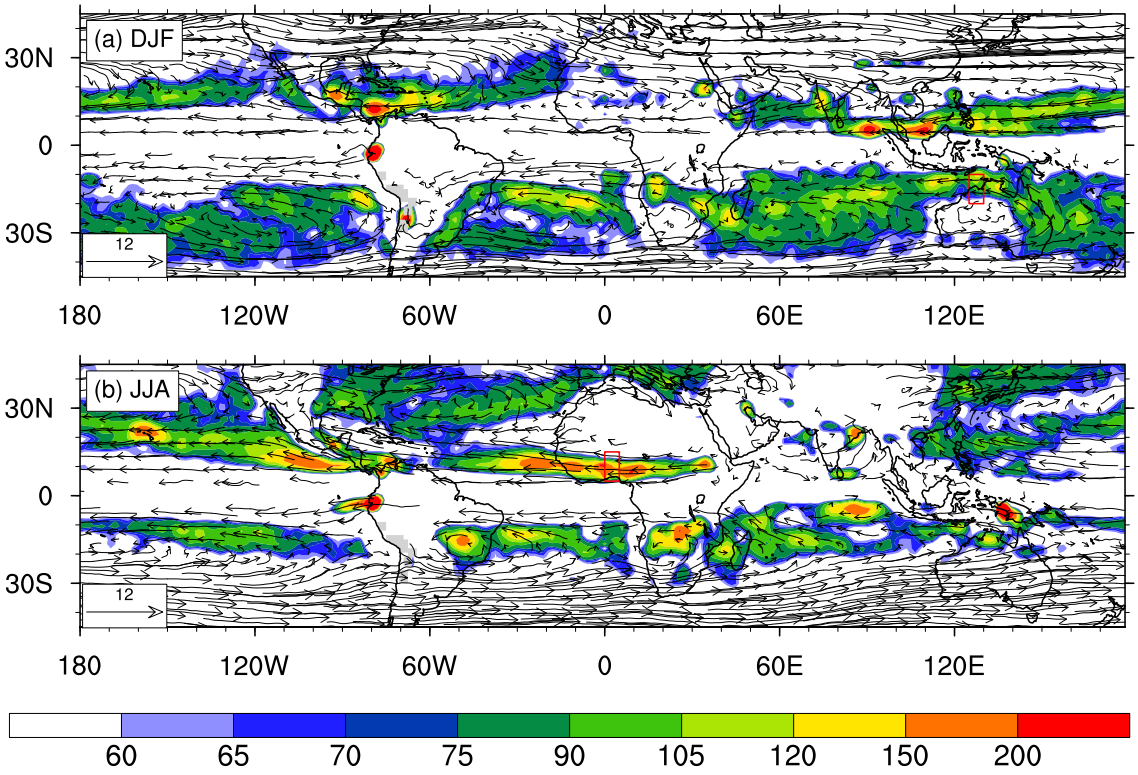

Figure 1 Climatological distribution of coherent PV maxima on 315 K isentropic surface (shaded) and their mean motion vectors. (a) DJF and (b) JJA. The unit for the color scale is the total number of coherent PV maxima in 1980–2009 per season, and the unit for the motion vector is m s^{-1}. Areas in which the 315 K mean isentropic surface lie below the topography are shaded gray and areas with fewer than 60 PV maxima are white. Two compositing regions are marked by two red boxes in DJF and JJA for the Australian and north African tropics respectively

4. Composite Synoptic Structure of Extreme Rainfall in the Australian Tropics

This section examines the composite structure of the synoptic systems responsible for extreme summer rainfall in a box (10-20°S, 125-130°E) over the Australian tropics from 1997 to 2009. There are 60 extreme rainfall days in DJF in this 13 year interval. Of those 60 days, 57 days (95 per cent) have either at least one coherent PV maximum at any time of the day within the compositing box or at least one coherent PV maximum less than five degrees to the east of it (the direction from which the coherent PV maxima mostly arrive). The other three days have coherent PV maxima just to the west of the compositing box. Also, of those 60 days, 16 are associated with a named tropical cyclone within 5 degrees of the compositing box.

The GPCP rainfall is the total rainfall in the 24 hour period beginning at 0000 UTC, whereas the ERA-Interim fields are six-hourly analyses. Composites of the PV and related quantities at each of these four reanalysis times on the extreme rain days are very similar although the amplitudes of the patterns vary. Only composites at 0600 UTC (1400 Local Time) are shown here as it is at this time that the convection is commonly most active in the tropics during summer (Yang and Slingo 2001).

	Proportion of air parcels originated poleward of 23.5 degree (%)		
	315 K	330 K	350 K
Australian tropics	49.4	51.3	38.4
North African tropics	25.3	34.6	6.3

Table 1 The maximum latitudes of air parcels during 5-day back trajectories

The composite PV on the 315 K isentropic surface (Fig. 2a) during extreme rain events in DJF has a maximum in the Australian tropics slightly to the east of the compositing box. This composite PV maximum is statistically significant at the 99% level. This composite maximum is connected to an elongated filament extending from the extratropics along the east coast. The pattern is similar to the PV tracking-based composite presented by Berry et al. (2012) even though their analysis did not differentiate between extreme and other types of rainfall. The isolated PV maximum is also slightly to the east of rainfall anomaly maximum which is also significantly higher than the random sample. This connection between the PV and rainfall will be discussed further in the following section. Although a positive rainfall anomaly associated with the extreme rain days (day 0) is relatively symmetric and decreases radially outward from the centre of the compositing box, the positive rainfall anomaly extends across the whole of tropical northern Australia.

There is a large area of anticyclonic PV on the 315 K isentropic surface over central Australia connected to the surface heat low, which is marked by high potential temperature at 900 hPa (Fig. 2b). This anticyclonic PV and the cyclonic PV in the compositing box (Fig. 2a) are separated by an easterly jet of about 6 m s^{-1} near 20°S on the 315 K isentropic surface. Panels a and b of Fig. 2 also show a cyclonic composite circulation at low levels (315 K and 900 hPa) to the east of the compositing box with a plume of moisture stretching over northern Australia.

The climatology at 0600 UTC in DJF is shown in Fig. 2c. In the mean, a PV trough extends along the eastern coast of Australia from the mid-latitudes although it is less distinct than in the composite. This PV trough is aligned from south-east to north-west and collocated with relatively high rainfall. The anticyclonic PV region associated with the heat low in the climatology is more extensive and intense than the corresponding region in the composite.

The key differences between the composite of extreme rain days and the climatology at 900 hPa (Fig. 2b, d) are that on days of extreme rain in the compositing box, the cyclonic circulation is significantly stronger in the eastern part of compositing box and a weak trough lies along 18–20°S, whereas in the climatology, tropical Australia is influenced by a monsoon trough along 15°S with southeasterlies on its poleward flank and westerly flow near the equator. The specific humidity in the Australian tropics in conditions of extreme rain is about 1 g kg^{-1} greater than normal (15 g kg^{-1} compared to 14 g kg^{-1}) and also significant over a large area in the Australian tropics (Fig. 2b). Although the potential temperature is about 1°C higher in the extreme rainfall composite compared to the climatology, it is not statistically significant. It is also consistent with the differences in low-level flow and rainfall anomaly discussed above.

Vertical cross sections of the extreme rainfall composites, taken along the central latitude and longitude of the compositing box on the day of extreme rainfall, are shown in Fig. 3. To the east of the rainfall maximum are two PV maxima, one in the mid levels at 400–500 hPa with values greater than 0.55 PVU and one in the low levels at 700 hPa with values of more than 0.45 PVU. The low-level PV maximum is consistent with the cyclonic circulation to the east of the compositing box, whereas the mid-level PV maximum is collocated with maximum rainfall anomaly (Fig. 2a). These two PV maxima are consistent also with the easterly jet near 20°S and the westerly jet near 8–10°S in the north-south cross section. The zero isotachs of the horizontal wind components are almost vertically aligned and pass through the PV maxima in both east-west and north-south cross sections showing a cyclonic circulation extending from the surface to upper-troposphere. Even though the PV anomalies lie in the low latitudes, the isentropes plotted in Fig. 3 bow slightly towards the PV maximum from above and below as predicted by theory first developed for mid- and high-latitudes (see Hoskins et al. 1985).

The composite structure of the diabatic heating is plotted in Figs. 3c and d). The evolution of the PV following fluid parcel is related to the diabatic heating rate through the expression

$$\frac{DP}{Dt} = -g\left(f+\zeta\right)\frac{\partial\dot{\theta}}{\partial p} \tag{2}$$

where P is the potential vorticity, defined by $P = (f\mathbf{k} + \nabla \wedge \mathbf{u}) . \nabla\theta/\rho$, $\mathbf{k}$ is the vertical unit vector, $\mathbf{u}$ is horizontal velocity vector, g is the acceleration due to gravity, f is the planetary vorticity, ρ is density, D/Dt is the time derivative following fluid parcels, ζ is the relative vorticity, $\dot{\theta}$ is the diabatic heating rate and p is the pressure. In this equation, the horizontal components of vorticity in the diabatic heating term are neglected as they are small compared to vertical component. The vertical gradient of the diabatic heating on the right hand side determines the vertical structure of the PV change following fluid parcels. For example, suppose the diabatic heating has a maximum in the middle troposphere. Then $\partial\dot{\theta}/\partial p$ is negative below the maximum heating and positive above it. As $-g\,(f + \zeta)$ is almost always positive in the Southern Hemisphere, the heating induces a cyclonic PV tendency following fluid parcels below the heating maximum and an anticyclonic tendency above that level.

The diabatic heating rate (Fig. 3c, d) has a maximum of 9–10 K day^{-1} in the middle and upper troposphere (300–500 hPa) with two centres on both sides of the mid-level PV maximum, one in the compositing box and one further east, near 130°E. The maximum diabatic heating in the compositing box is presumably generated by the extreme rainfall in the box, whereas the maximum to the east may be related to the low-level (700 hPa) cyclonic PV (Figs. 2b and 3a). The vertical gradient of the diabatic heating associated with deep convection generates cyclonic PV following fluid parcels below the level of maximum heating. The maximum diabatic heating in north-south cross section (Fig. 3d) is a single maximum, located higher (about 300–400 hPa) and slightly to the south of the PV maximum. Taking both cross-sections together, the generation of PV through diabatic heating is largely westward of the coherent PV maximum where the convection and rainfall are most intense. In so far as can be determined from the 1.5 degree resolution reanalysis, these vertical structures of diabatic heating, horizontal wind and PV are similar to the MCSs described by Chen and Frank (1993) and Houze (2004) in which the region of maximum PV and heating are found in the middle troposphere and the strongest cyclonic circulation lies below them (Figs. 21 and 25 in Houze 2004).

Another near-surface maximum in the heating rate in the extratropics is related to the surface heat low which lies poleward of the easterly jet (20–30°S, about 700 hPa). This near-surface maximum in the heating rate is also consistent with the anticyclonic PV generation above the surface (Fig. 3c) and the PV anticyclone on the 315 K isentropic surface (Fig. 2a).

Time-lagged composites of the PV field on the 315 K isentropic surface and the rainfall anomaly from four days before (day -4) to four days after (day +4) the extreme rain day are plotted in Fig. 4. The evolution shows a connection to the midlatitudes through a filament along the east coast of Australia, and the subsequent advection of cyclonic PV toward the Northern Territory and then north-west Australia. Four days before the extreme rain, an elongated PV tongue lies over north-east Australia on the 315 K isentropic surface, aligned from south-east to north-west and a large area of anticyclonic PV lies over the heat low which are similar to the climatology shown in Fig. 2c. On this day, there is a statistically significant PV maximum in western Australia, although it does not cause any significant rainfall anomaly over land.

Two days prior to the extreme rainfall (Fig. 4b), an isolated and statistically significant PV maximum forms about 5 degrees to the east of the compositing box, near (16°S, 133°E) with a statistically significant increase in rainfall of 8 mm day^{-1} equatorward. This maximum then intensifies and moves toward the compositing box over the next two days as discussed in the previous section in connection with the PV budget. On the extreme rain day (Fig. 4c), the rainfall anomaly is more than 30 mm day^{-1} in the compositing box. Over the next few days (Fig 4d, e), the composite PV maximum propagates to the south-west along the north-western Australian coast producing statistically significant positive anomalous rainfall in western Australia and statistically significant changes in the PV field, especially at low levels. The rainfall anomaly over western Australia increases to 3–6 mm day^{-1} on day +4 (Fig. 4e), which is a statistically significant increase as the summer rainfall in this region is low. As the composite PV maximum moves into the region, the anticyclonic PV over the heat low on the 315 K isentropic surface is almost completely absent by day +4. The path of the composite PV maximum is similar to that of monsoon depressions reported previously (e.g. Hell and Smith 1998, Berry et al. 2012). Figure 4 also shows that following the extreme rainfall over northern Australia, the area of positive anomalous rainfall expands southward. The broad area of enhanced rainfall moves inland from around 10–12°S on day -4 to around 18–20°S on day +4.

The time-lagged rainfall and PV composites identify a southward movement of the statistically significant positive rainfall anomaly and PV maximum after the day of extreme rainfall. This suggests that the large-scale conditions could be substantially modified in the monsoon region in the wake of an extreme rainfall event. Figure 5 shows the frequency of the objectively detected ITCZ as defined by Berry and Reeder (2013), which is used here as a proxy for the monsoon trough. The first three panels show different snapshots (at day -4, day 0 and day +6) and the bottom right panel is the latitude-time distribution of the frequency of the monsoon trough averaged over the longitudes 120°E–135°E. Four days before the extreme rainfall event (Fig. 5a), the trough frequency is largest over the ocean near 12°S. This maximum in the trough frequency is

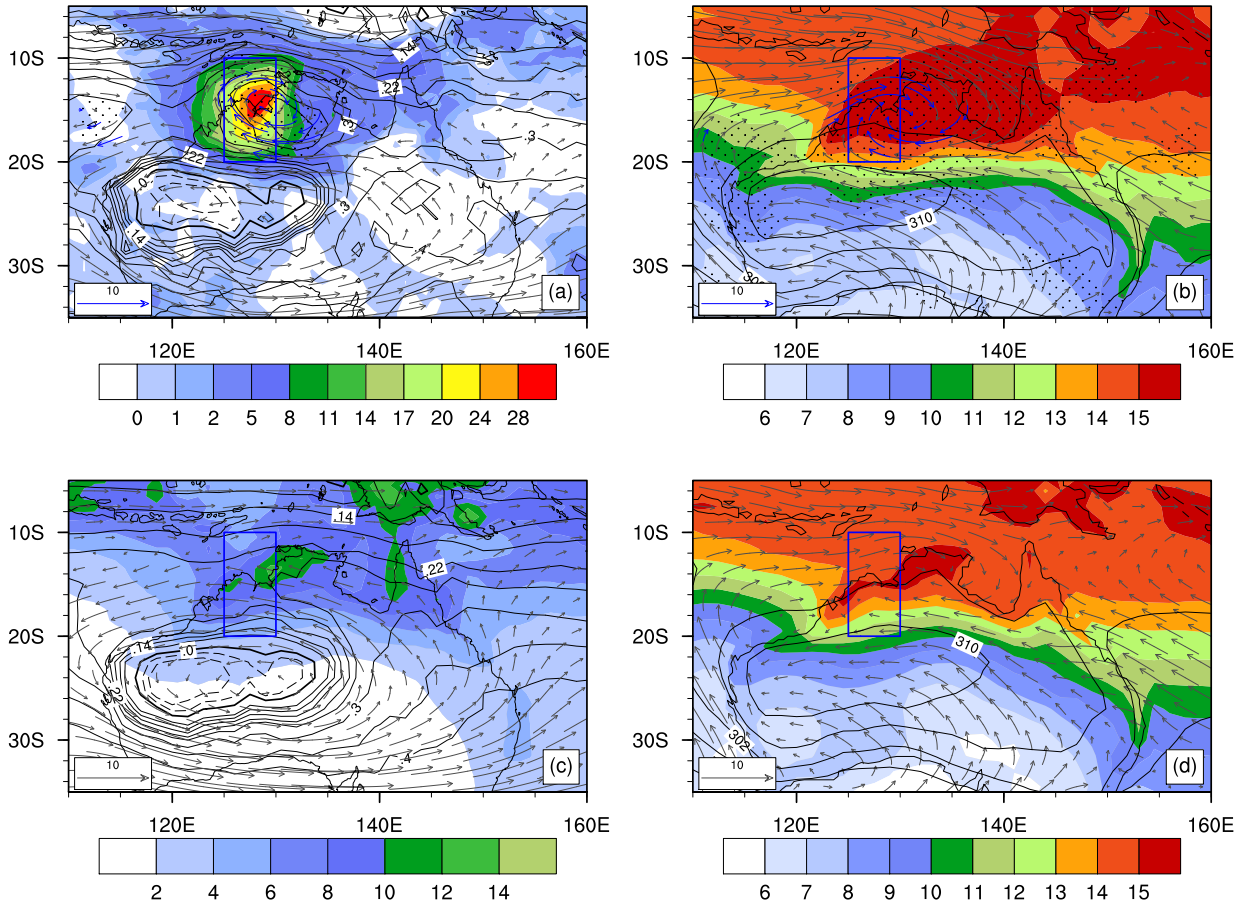

Figure 2 Composite structure of extreme rain events in the compositing box 10°S–20°S, 125°E–130°E over northern Australia in DJF from December 1996 to February 2009 (panels a and b) and the climatological distribution (panels c an d). (a) Composite structure of the 315 K PV (contours, dashed negative, bold line zero, stippled statistically significant, PVU), daily rainfall anomaly (shaded, mm day^{-1}), and wind for statistically significant, high relative vorticity area on 315 K isentropic surface (vectors, m s^{-1}) at 0600 UTC on extreme rain days. Areas of negative rainfall anomaly are white. (b) The specific humidity (shaded, stippled statistically significant, g kg^{-1}), potential temperature (black contours, K) and wind for statistically significant, high relative vorticity area on 900 hPa (vectors, m s^{-1}) at 900 hPa. Areas with specific humidity smaller than 6 g kg^{-1} are white. (c) Climatological (1997–2009) daily rainfall in DJF (shaded, mm), and 0600 UTC PV (contour, dashed negative, bold line zero, PVU) and wind (vector, m s^{-1}). (d) Climatological 0600 UTC specific humidity (shaded, g kg^{-1}), and potential temperature (contour, K) and wind (vector, m s^{-1}).

consistent with the composite elongated PV filament over north and east Australia as shown in Fig. 4a. Another maximum of the PV in the subtropics near 20–22°S is linked to the heat low in central Australia. On the day of extreme rainfall in the compositing box (Fig. 5b), both frequency maxima increase (meaning more troughs are identified in the regions on these days). At the same time, the tropical trough moves slightly southward towards central Australia. Six days after the extreme rain (Fig. 5c), the trough frequency in the tropics decreases markedly while the frequency of the troughs in the subtropics increases markedly. This result is consistent with the rainfall composite in the previous section and the results of Davidson et al. (1983) (see especially their Fig. 9) in which the positive rainfall anomaly regions move inland, often hearalding the monsoon onset in Australia.

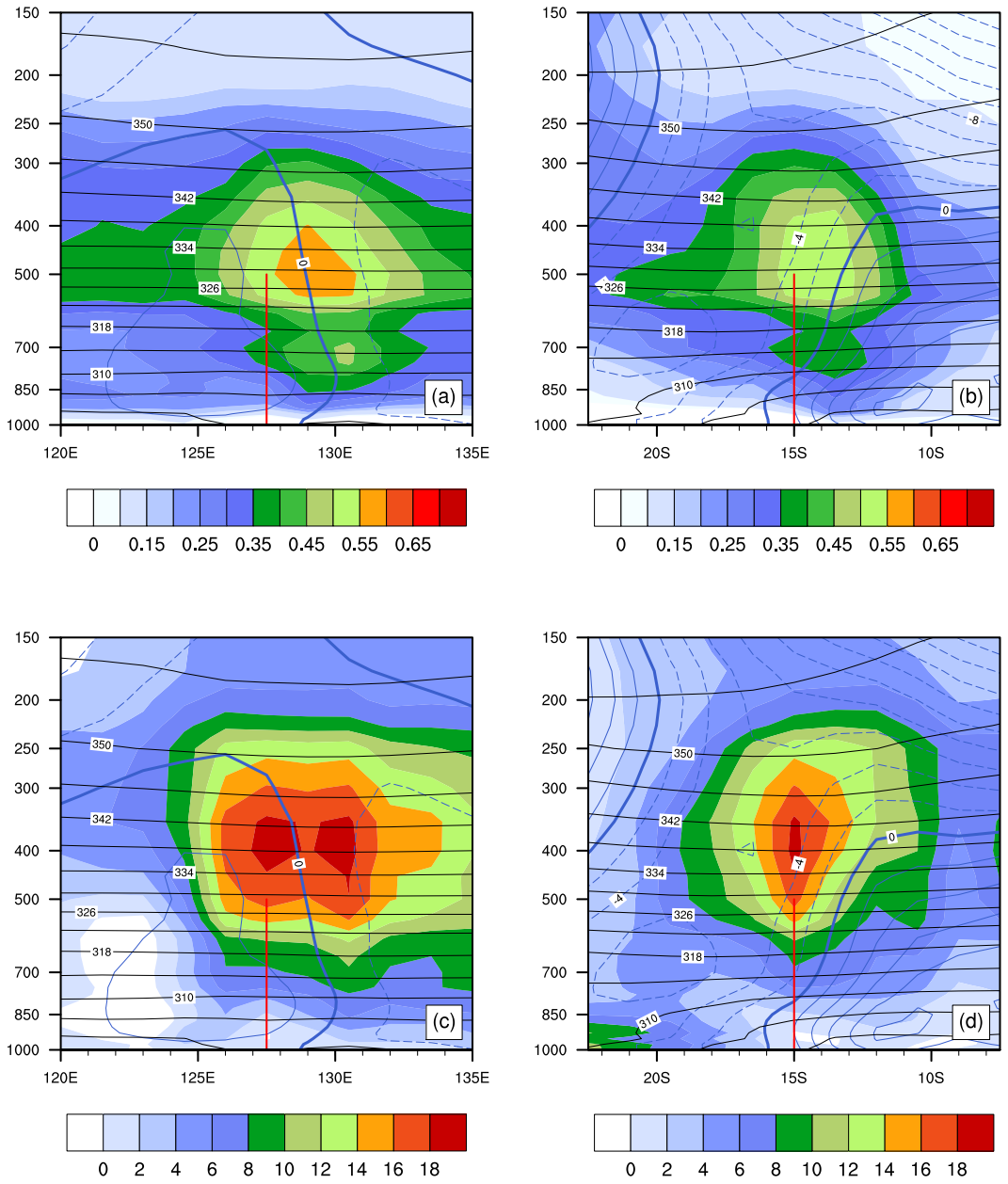

Figure 3 (a) East-west cross section along 15°S showing the centre longitude of the compositing box (red vertical line), PV (shaded, multiplied by -1 for SH, PVU), potential temperature (black contour, K) and meridional wind (blue contours every 2 m s^{-1}, dashed negative, bold line zero). (b) North-south cross section along 130°E showing the centre latitude of compositing box (red vertical line), PV (shaded, multiplied by -1 for SH, PVU) and potential temperature (black contours, K) and zonal wind (blue contours, every 2 m s^{-1}, dashed negative, bold line zero, m s^{-1}). (c) Similar to (a) but for diabatic heating (shaded, K day^{-1}). (d) Similar to (b) but for diabatic heating (shaded, K day^{-1}).

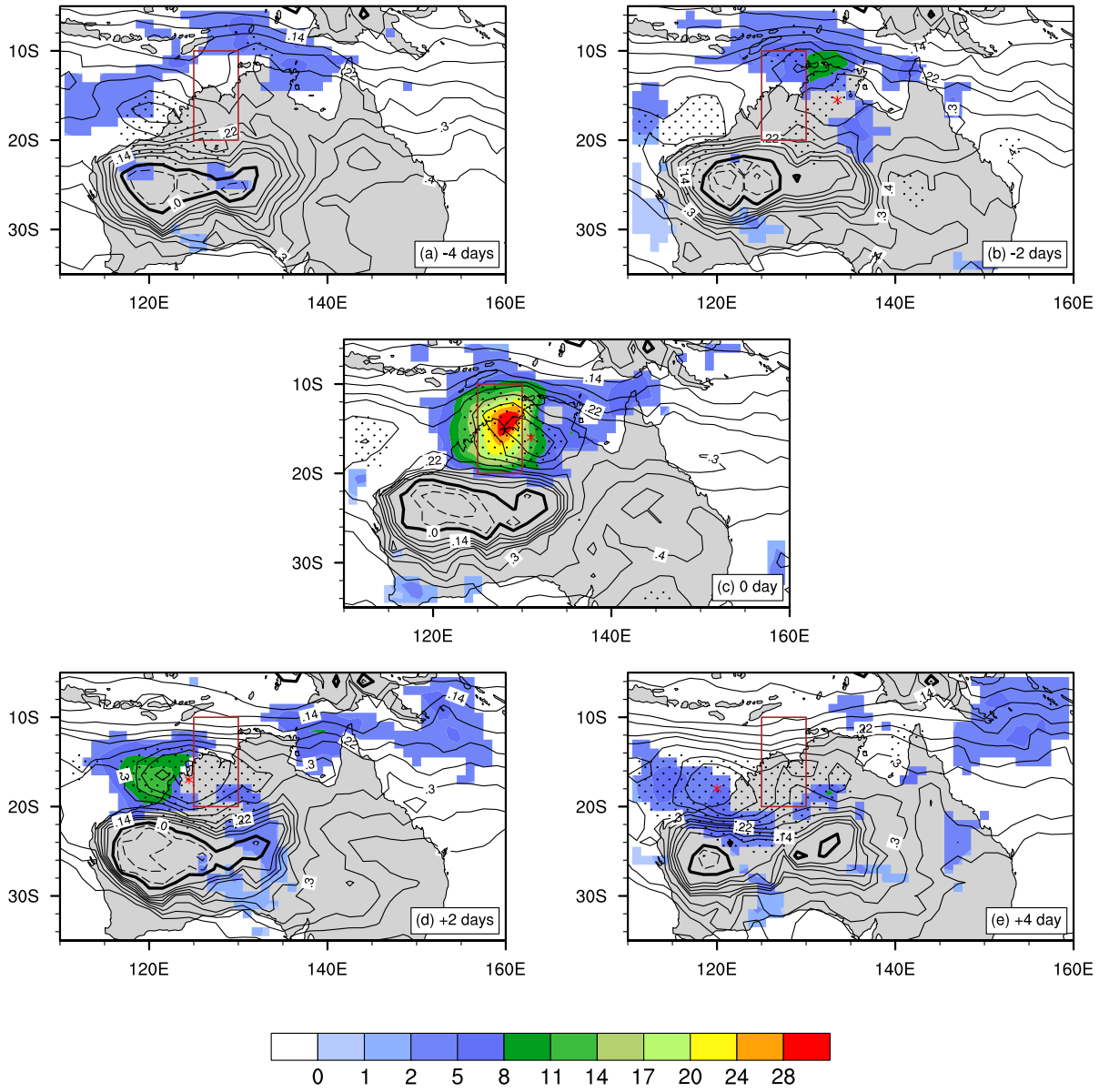

Figure 4 The composite evolution of extreme rainfall in the compositing box from -4 to +4 days showing the significant rainfall anomalies (shaded, mm day^{-1}) and the associated 315 K PV field (contours, bold line zero, dashed negative, black stippled statistically significant, PVU) and coherent PV maximum (red asterisk).

5. Composite Synoptic Structure of Extreme Rainfall in the North African Tropics

The compositing box over the north African tropics is chosen because, like northern Australia, it is an area where the frequency of coherent PV maxima on the 315 K surface during summer is high (Fig. 1). Both regions have broad oceans equatorward and extensive deserts poleward. The juxtaposition of the ocean and desert produces a reversal in the mean north-south temperature gradient and, through thermal wind, a low level easterly jet. Unlike tropical northern Australia, tropical north Africa is not fed with a relatively large meridional flux of coherent PV maxima (Fig. 1), prompting the current investigation into the degree of similarity between the extreme-rain producing systems in the two regions.

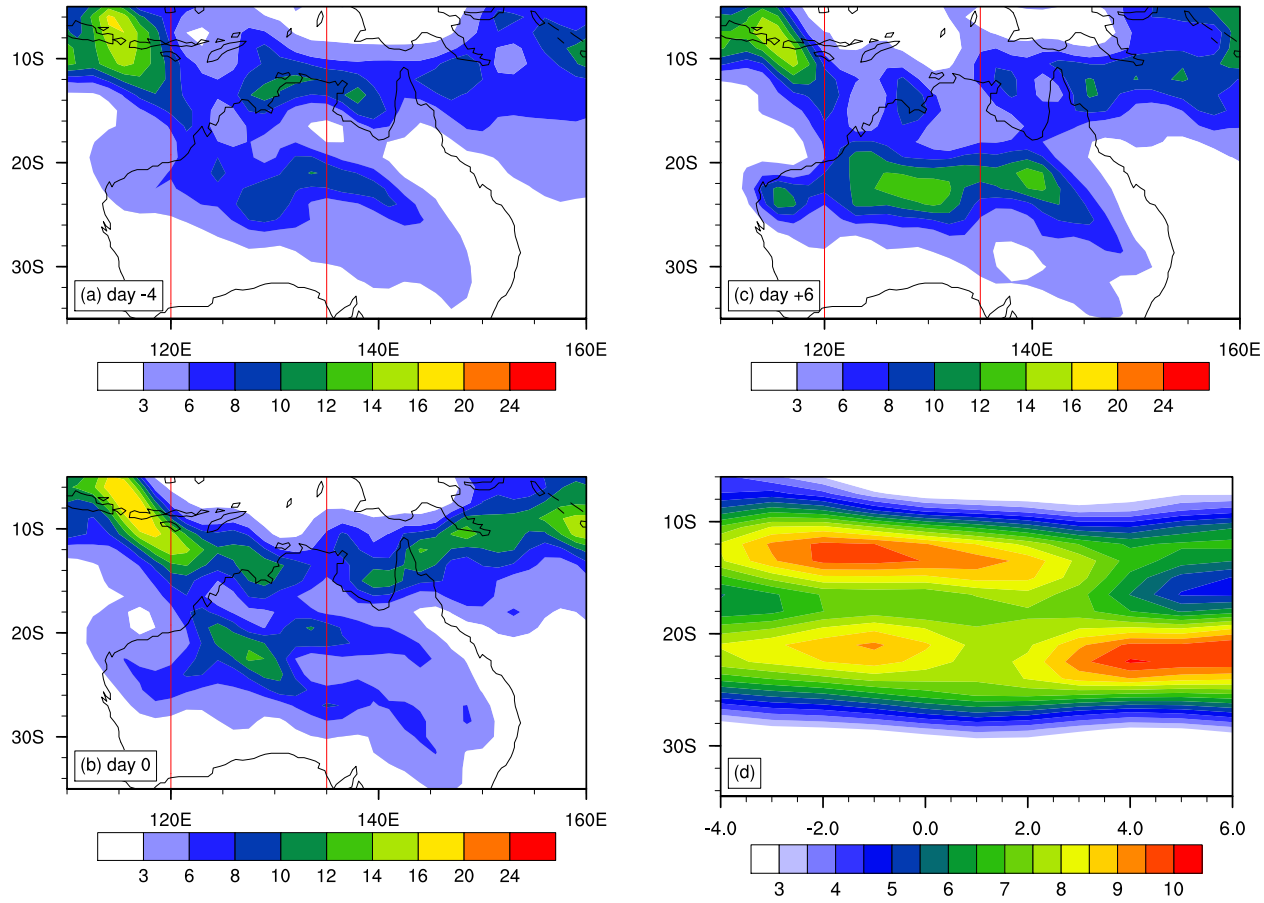

Figure 5 Frequency of monsoon troughs (shaded) (a) 4 days before an extreme rainfall event, (b) on the day of extreme rain and (c) 6 days after the extreme rain day in DJF over northern Australia from 1997 to 2009. Areas with fewer than 3 troughs per 13 years (1997–2009) are white. The vertical red lines mark the longitude interval (120–135°E) for averaging. (d) The number of monsoon trough (shaded) averaged over the longitude interval as a function of latitude and time, from four days before to six days after extreme rain events.

Like the extreme rainfall in the Australian compositing region, 50 out of 61 extreme rain days (82 per cent) in the north African tropics are associated with either a coherent PV maximum in the compositing box (at any time of the day) or a coherent PV maximum less than 5 degrees to the east (upstream) of the box. The composite of 61 extreme rain days in JJA in the compositing box from 5-15°N, 0-5°E over the north African tropics at 1200 UTC (1200 Local Time) shows many similarities with the Australian tropics (see the earlier discussion in the Section 4). Here 1200 UTC is analyzed as it is close to the time of the highest diabatic heating rates in the box. Although not shown, the composite PV at 1200 UTC has the coherent PV maximum lying just to the east of the box, with the largest rainfall in the box. Six hours later at 1800 UTC the composite coherent PV maximum lies in the box with the maximum rainfall slightly west of the box.

The composite PV on the 315 K isentropic surface and the climatology at 1200 UTC in JJA are shown in Fig. 6. Comparing the two composites for the north African and Australian tropics, both have broad areas of statistically significant positive rainfall anomaly downstream of a significant coherent PV maximum at 315 K. Figures 2b and 6b both show very strong gradients in specific humidity along 20°S and 18°N separating moist tropical, monsoon air from dry, desert air. Both show the low-level easterly jets documented by Dickinson and Molinari (2000) in their study of sign reversals in the meridional

PV gradient over Africa and Australia.

There are, however, three important differences in the large-scale structure between the composites in two regions. First, the 900 hPa composite in the north African tropics shows a monsoon trough along 16–20°N which is known as Intertropical Front (see e.g. Lélé and Lamb 2010). This trough separates the warm moist monsoon southwesterly flow from hotter and drier northeasterly wind from Sahara desert and the intensity of the wind is not significantly different to the random sample. In the Australian tropics, a shorter, semi-permanent trough lies around 20°S (Fig. 2b). Moreover, the Australian trough is stronger with a significantly stronger cyclonic circulation to the east of the compositing box in the tropics. Second, the amplitude of the PV in the north African composite is less than that in the Australian tropics (the largest closed contour in Fig. 2a for the Australian tropics is about 0.40 PVU, whereas in Fig. 6a it is 0.22 PVU). Third, the rainfall in the north African tropics is less than that over northern Australia although as a percentage of the climatological amount, the anomaly is larger. The mean rainfall in the north African tropics is relatively low, about 4–5 mm day^{-1} in the compositing box in JJA, yet the rainfall anomaly is more than 15 mm day^{-1}, which is about four times the mean rainfall. In the Australian tropics, this factor is about two.

Although the cross section for the north African tropics (Fig. 7) also shows a PV maximum at around 500 hPa in the eastern part of the compositing box near 6°E, it is weaker (0.35 PVU compared to 0.5 PVU in Fig. 3) and it does not have a double PV structure as in the Australian composite cross sections (Fig. 3).

Similar to the northern Australia composite, the east-west cross section of the composite diabatic heating rate in the north African composite shows two maxima, both on the east of the compositing box and about five degrees from each other. They lie on each side of the PV maximum described above. In comparison with Figs. 3c and d, the maximum in the diabatic heating rate in the north African tropics is both weaker and closer to the surface than that in the Australian tropics (10–12 K day^{-1} at 500 hPa compared to 14–16 K day^{-1} at 400 hPa). Moreover, the diabatic heating maximum lies slightly further ahead of the PV maximum compared to the Australian composite. This displacement is consistent with the higher propagation speed of the coherent PV maximum in north Africa. The maximum diabatic PV tendency lies largely over the continent, on the south-western side of the PV maximum where organized deep convection is most frequent (see e.g. Laing and Fritsch 1997). As in the Australian composite, the convection in tropical north Africa is preferentially located on the equatorward side of the easterly jet.

The surface heating rate over the Sahara is higher and the desert extends further equatorward than the desert in Australia. The associated mixed layer over the Sahara is also deeper than that over the desert in central Australia (the anticyclonic PV extends to 700 hPa in Fig. 7b compared to 850 hPa Fig. 3b).

The zero isotachs of the u and v-components of the wind in the north African composites shown in Figs. 7a and c are markedly different to those in the northern Australian composite. In the north Africa composites, these contours separate the westerly wind at low levels from the easterly winds at upper levels. They are horizontal aligned around 700–850 hPa. These characteristics of the extreme rainfall composite in tropical north Africa are similar to easterly waves (Pytharoulis and Thorncroft 1999) which have shallow monsoon westerlies at low levels and an easterly jet in the mid-troposphere.

The above analysis for the north African tropics underscores the connection between extreme rainfall and synoptic-scale cyclonic PV maxima. Like the cases of extreme rainfall in tropical Australia, the generation of PV through diabatic heating lies largely to the west of the coherent PV maximum, collocated with the maximum convection and rainfall, although the separation between the PV anomaly and maximum diabatic heating is larger in the north Africa than in northern Australia.

The time-lagged composites of the PV field on the 315 K isentropic surface and the rainfall anomalies for tropical north Africa are plotted in Fig. 8. Two days before the extreme rainfall event, a PV trough lies along the north African tropics with several embedded coherent PV maxima (Fig. 8a). The rainfall anomaly is negative over the compositing box and slightly positive on the west African coast, near 10°W. A coherent PV maxima located near 20°E moves westward to 16°E by day -1 (Fig. 8b). The positive rainfall anomaly on the eastern side of the compositing box increases significantly by day -1 at the leading edge of the westward-moving coherent PV maximum.

On the extreme rain day, the composite PV maximum lies just to the east of the compositing box with a statistically significant increase in the rainfall anomaly, up to 18 mm day^{-1} (Fig. 8c). One day later, the statistically significant, high PV maximum and associated significant positive rainfall anomaly continue to move westward and the rainfall anomaly in the compositing box falls quickly, becoming negative (Fig. 8d). Two days after the extreme rain event (Fig. 8e), the PV and rainfall anomaly

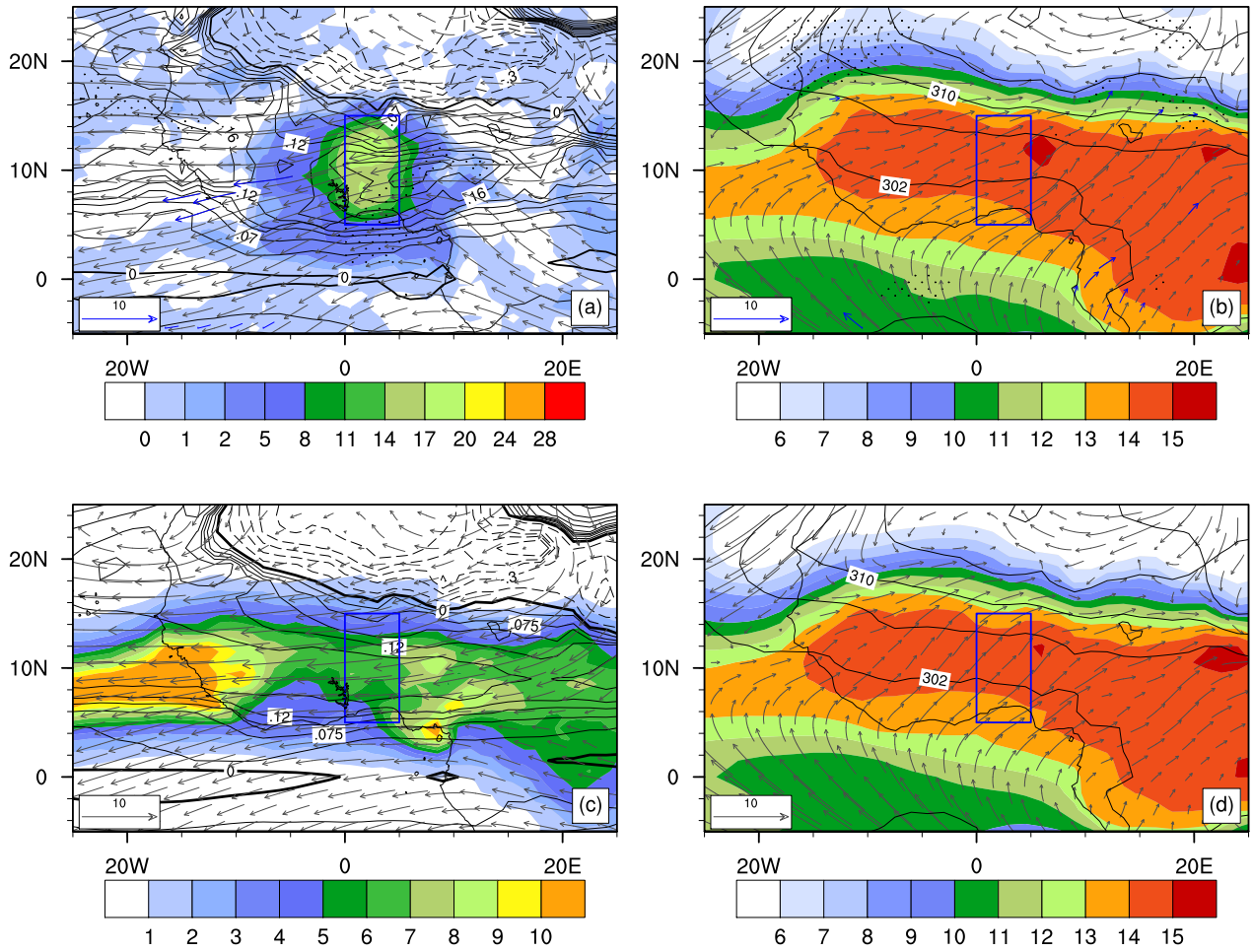

Figure 6 Composite structure of extreme rain events in the compositing box 5°N–15°N, 0°E–5°E over north Africa in JJA from June 1997 to August 2009 (panels a and b) and the climatological distribution (panels c an d).(a) Composite structure of the 315 K PV (contours, dashed negative, bold line zero, stippled statistically significant, PVU), daily rainfall anomaly (shaded, mm day^{-1}), and wind for statistically significant high relative vorticity area on 315 K isentropic surface (vectors, m s^{-1}) at 1200 UTC on extreme rain days. Areas of negative rainfall anomaly are white. (b) The specific humidity (shaded, stippled statistically significant, g kg^{-1}), potential temperature (black contours, K) and wind for statistically significant, high relative vorticity area on 900 hPa (vectors, m s^{-1}) at 900 hPa. Area with specific humidity smaller than 6 g kg^{-1} are white. (c) Climatological (1997–2009) daily rainfall in JJA (shaded, mm), and 1200 UTC PV (contour, dashed negative, bold zero, PVU) and wind (vector, m s^{-1}). (d) Climatological 1200 UTC specific humidity (shaded, g kg^{-1}), and potential temperature (contour, K) and wind (vector, m s^{-1}).

fields are similar to those two days before the event; specifically there is a negative rainfall anomaly in the compositing region, with another PV maxima forming to the east.

The frequency of the monsoon trough on day 0 and the latitude-time distribution from day -4 to day +6 are shown in Fig. 9. On the day of extreme rainfall, the monsoon trough is located near 20°N, to the north of the compositing box. The latitude-time plot of averaged frequency over longitudes 5°W-10°E shows a persistent trough at 20°N and a less frequent trough

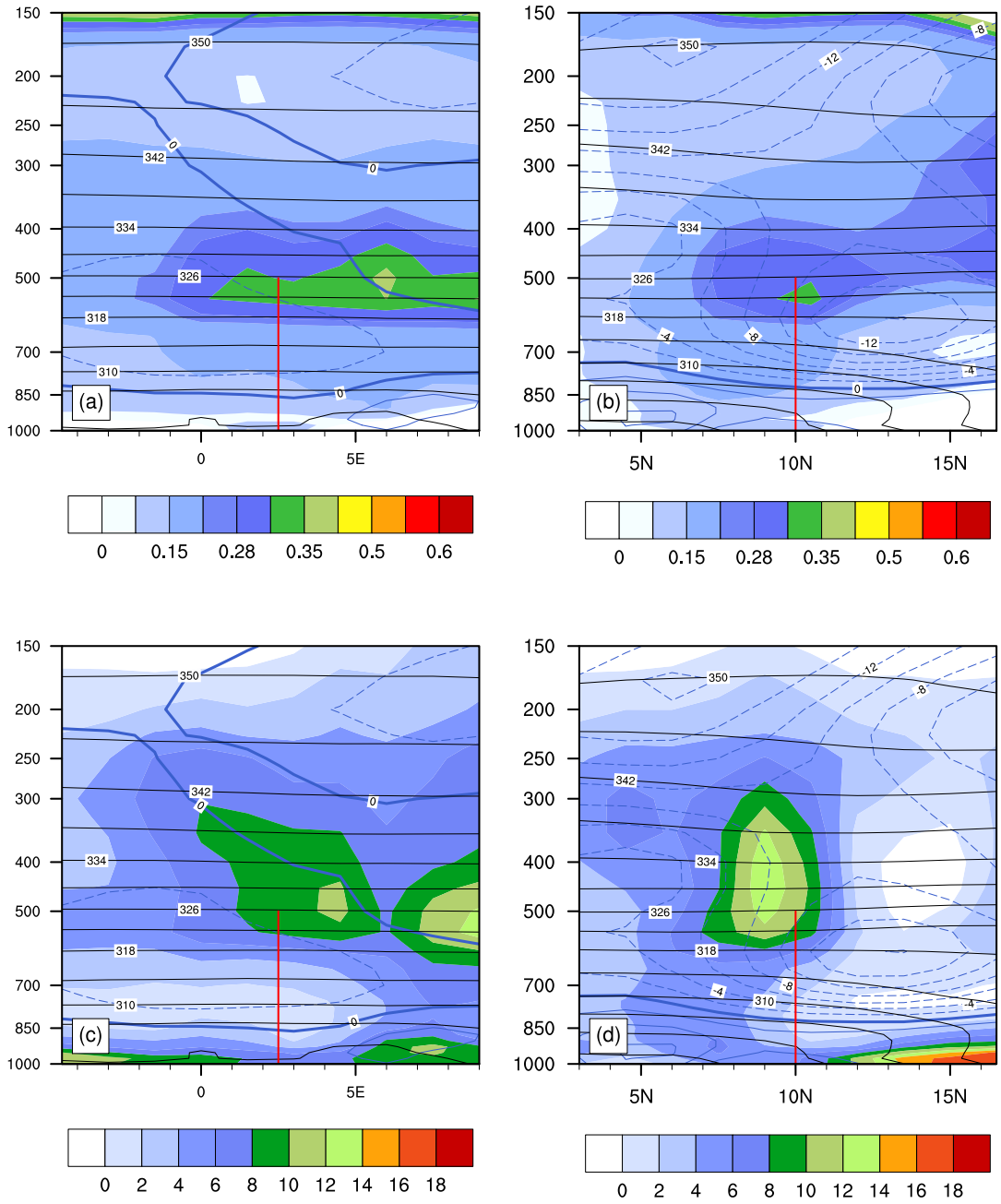

Figure 7 (a) East-west cross section along 7.5°N showing the centre longitude of the compositing box (red vertical line), PV (shaded, PVU), potential temperature (black contours, K) and meridional wind (blue contours every 2 m s^{-1}, dashed negative, bold line zero). (b) North-south cross section along 2.5°E showing the centre latitude of compositing box (red vertical line), PV (shaded, PVU), potential temperature (black contours, K) and zonal wind (blue contours, every 2 m s^{-1} dashed negative, bold line zero, m s^{-1}). (c) Similar to (a) but for diabatic heating (shaded, K day^{-1}). (d) Similar to (b) but for diabatic heating (shaded, K day^{-1}).

near 8°N. The extreme invariance of the monsoon trough pattern in periods of extreme rainfall (Fig. 9) indicates that the basic state in north Africa is much less affected by individual transient disturbances than the northern Australian basic state. Nonetheless, there are examples of individual MCSs producing a marked poleward shift in the position of the north African

monsoon trough (for example, see Flamant et al. 2009).

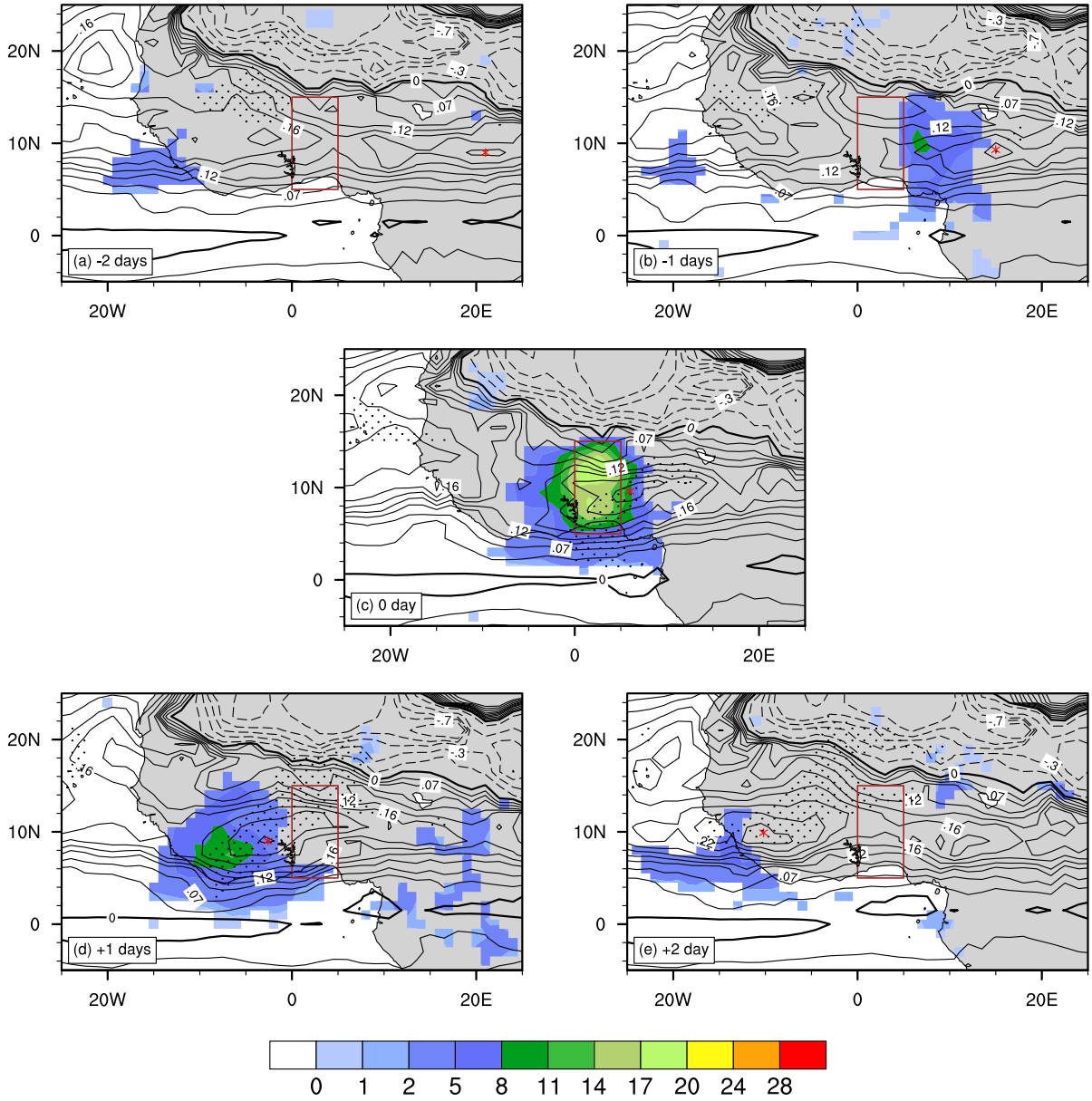

Figure 8 The composite evolution of extreme rainfall in the compositing box from -2 to +2 days showing the significant rainfall anomalies (shaded, mm day^{-1}) and the associated 315 K PV field (contours, bold line zero, dashed negative, black stippled statistically significant, PVU) and coherent PV maximum (red asterisk).

6. Discussion and Conclusions

A global climatology of coherent PV maxima in DJF and JJA has been constructed using the objective PV maximum tracking technique of Berry et al. (2012). In the tropics, areas with a high number of coherent PV maxima are those in which the frequency of mesoscale convective complexes is also high (Laing and Fritsch 1997), especially in north Africa in JJA and northern Australia in DJF. A detailed comparison between these two regions is made because they are geographically and climatologically similar. In particular, in both regions oceans lie equatorward and extensive deserts lie poleward, a juxtaposition that produces a reversal in the mean north-south temperature gradient and, through thermal wind, a low level easterly jet. Consequently, it is of interest to understand the degree to which the extreme-rain producing systems in each region are

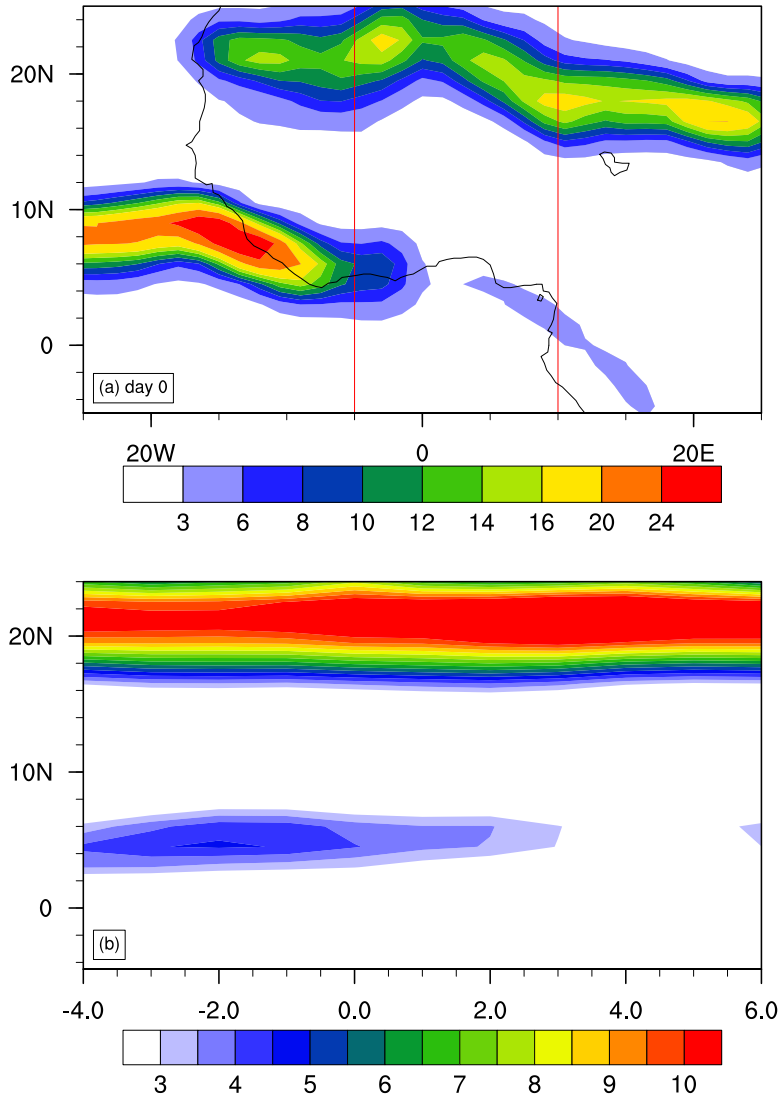

Figure 9 (a) Frequency of monsoon troughs (shaded) for the day of extreme rain events (day 0) in JJA over tropical north Africa from 1997 to 2009. The vertical red lines mark the longitude interval (5°W–10°E) for averaging. (b) The number of monsoon trough (shaded) averaged over the longitude interval as a function of latitude and time, from four days before to six days after extreme rain events.

similar.

The transport of coherent PV maxima from the extratropics to the tropics is especially pronounced along eastern Australia in DJF. Between 6–12 per cent of the 315 K and 330 K isentropic coherent PV maxima crossing the compositing box in northern Australia are first detected in the extratropics. Because coherent PV maxima are isolated PV anomalies, the tracking algorithm under estimates the degree to which they are connected to the midlatitudes through PV filaments, for example. The constituent air parcels for more than half of all coherent PV maxima that cross the compositing box in the Australian tropics have their origins in the extratropics. The proportion of the coherent PV maxima with extratropical origins in the north African tropics is smaller than that in the Australian tropics; in the tropical north Africa, coherent PV maxima originate in the tropics, and are mostly linked to organized deep convection in central or eastern Africa. No coherent PV maxima on the 315 K or 350 K isentropic surfaces are first detected outside the tropics, whereas less than 4 per cent of those on the 330 K isentropic surface

are first detected in the extratropics. However, five-day back trajectory calculations show that 34 per cent of the air parcels near the 330 K coherent PV maxima are extratropical in origin.

Composites based on extreme rain days, defined by the top 5 per cent of daily GPCP rainfall for those two regions, show that the composite fields for the north African tropics are broadly similar to those for the Australian tropics, although the absolute amplitude of PV maximum over north Africa is weaker and the scale of the disturbance is larger. In both regions, the largest positive rainfall anomaly occurs ahead of the PV maxima and these rainfall anomalies and PV maxima are significantly larger than the mean rainfall and PV over the respective regions in respective seasons.

Extratropical PV filaments are drawn equatorward along the Australian east coast, eventually breaking into isolated, coherent PV maxima that promote convection and rain ahead of them. The associated latent heating produces cyclonic PV at low levels and anticyclonic aloft. This sequence of events is evident in the composite for the extreme rain events. Presumably, diabatic heating is an important contributor to the evolution of the PV field during the extreme rainfall days, with the generation of PV through diabatic heating lying ahead of the moving coherent PV maxima.

The vertical structure of the PV fields in the two regions are similar in general, with a cyclonic PV maximum in the mid-troposphere located just below the maximum of diabatic heating. This PV maximum is similar to the mid-troposphere vortex generated by MCSs (see e.g. Bartels and Maddox 1991, Chen and Frank 1993, Fritsch et al. 1994, Houze 2004). The composite horizontal wind structures, however, reveal that the extreme rainfall composites in the Australian tropics are similar MCSs, whereas in the north African tropics, they are similar to the easterly waves.

In the north African tropics, coherent PV maxima are generated in the tropics, progress westward, and promote convection and rainfall ahead the coherent PV maxima, consistent with the composite African Easterly Waves structure (e.g. Carlson 1969). This highly repeatable picture over the north African tropics is reflected in the highly persistent pattern of the monsoon trough frequency. It appears that individual transient disturbances affect the mean state over north Africa much less than they affect the mean state of northern Australia. In Australia, the extreme rain event is evidently a precursor to large-scale changes in the circulation, e.g. the displacement of the monsoon trough towards central Australia (see e.g. Davidson et al. 1983, Berry et al. 2012).

This and previous work (e.g. Berry et al. 2012) emphasize that rainfall, and especially extreme rain in the Australian and north African tropics, is strongly linked to coherent PV maxima. It also underscores the role of a synoptic forcing in the development of extreme rainfall. The work suggests that properly simulating these dynamical process is essential for the correct prediction of extreme rainfall in numerical weather prediction and climate models. The influence of the Madden-Julian Oscillation, other tropical waves and the state of the monsoon on the frequency and structure of coherent PV maxima are topics of continuing research.

Acknowledgements

The authors thank Noel Davidson and an anonymous reviewer for their insightful comments and suggestions. LH was supported by an AusAid Scholarship. GJB and JS were supported by the Australian Research Council Grant FS100100081. Reanalysis data used in this study were provided by the ECMWF, and GPCP rainfall data were obtained from NASA Goddard Earth Sciences Data and Information Service Center.

References

Bartels, D.L. and Maddox, R.A. 1991. Midlevel cyclonic vortices generated by mesoscale convective systems. *Monthly Weather Review*, 119(1), 104–118. ISSN 0027-0644.

Berry, G. and Reeder, M.J. 2013. Objective identification of the intertropical convergence zone: Climatology and trends from the ERA-Interim. *Journal of Climate*, 27(5), 1894–1909.

Berry, G.J., Reeder, M.J. and Jakob, C. 2012. Coherent synoptic disturbances in the Australian monsoon. *Journal of Climate*, 25(24), 8409–8421.

Berry, G.J. and Thorncroft, C. 2005. Case study of an intense African easterly wave. *Monthly Weather Review*, 133(4), 752–766.

Berry, G.J. and Thorncroft, C.D. 2011. African easterly wave dynamics in a mesoscale numerical model: The upscale role of convection. *Journal of the Atmospheric Sciences*, 69(4), 1267–1283.

Carlson, T.N. 1969. Some remarks on African disturbances and their progress over the tropical Atlantic. *Monthly Weather Review*, 97, 716–726.

Chen, S.S. and Frank, W.M. 1993. A numerical study of the genesis of extratropical convective mesovortices. Part I: Evolution and dynamics. *Journal of the Atmospheric Sciences*, 50(15), 2401–2426.

Davidson, N.E. and Holland, G.J. 1987. A diagnostic analysis of two intense monsoon depressions over Australia. *Monthly Weather Review*, 115(2), 380–392.

Davidson, N.E., McBride, J.L. and McAvaney, B.J. 1983. The onset of the Australian monsoon during winter MONEX: Synoptic aspects. *Monthly Weather Review*, 111(3), 496–516.

Dickinson, M. and Molinari, J. 2000. Climatology of sign reversals of the meridional potential vorticity gradient over Africa and Australia. *Monthly Weather Review*, 128(11), 3890–3900.

Efron, B. and Tibshirani, R.J. 1993. An Introduction to the Bootstrap. Chapman and Hall, New York.

Flamant, C., Knippertz, P., Parker, D.J., Chaboureau, J.P., Lavaysse, C., Agusti-Panareda, A. and Kergoat, L. 2009. The impact of a mesoscale convective system cold pool on the northward propagation of the intertropical discontinuity over west africa. *Quarterly Journal of the Royal Meteorological Society*, 135(638), 139–159.

Fritsch, J.M., Murphy, J.D. and Kain, J.S. 1994. Warm-core vortex amplification over land. *Journal of the Atmospheric Sciences*, 51(13), 1780–1807. ISSN 0022-4928.

Gill, J. 1999. The insignificance of null hypothesis significance testing. *Political Research Quarterly*, 52(3), 647–674.

Godbole, R.V. 1977. The composite structure of the monsoon depression. *Tellus*, 29(1), 25–40. ISSN 2153-3490.

Hell, R.M. and Smith, R.K. 1998. A monsoon depression over northwestern Australia. Part I: Case study. *Australian Meteorological Magazine*, 47(1), 21–40.

Hoskins, B.J., McIntyre, M.E. and Robertson, A.W. 1985. On the use and significance of isentropic potential vorticity maps. *Quarterly Journal of the Royal Meteorological Society*, 111(470), 877–946.

Houze, R.A. 2004. Mesoscale convective systems. *Reviews of Geophysics*, 42(4), RG4003.

Huffman, G.J., Adler, R.F., Morrissey, M.M., Bolvin, D.T., Curtis, S., Joyce, R., McGavock, B. and Susskind, J. 2001. Global precipitation at one-degree daily resolution from multisatellite observations. *J. Hydrometeor*, 2(1), 36–50.

Johnson, D.H. 1999. The insignificance of statistical significance testing. *Journal of Wildlife Management*, 63(3), 763–772.

Kong, Q. and Zhao, S. 2010. Heavy rainfall caused by interactions between monsoon depression and middle-latitude systems in Australia: a case study. *Meteorology and Atmospheric Physics*, 106(3-4), 205–226. ISSN 0177-7971.

Laing, A.G. and Fritsch, J.M. 1997. The global population of mesoscale convective complexes. *Quarterly Journal of the Royal Meteorological Society*, 123(538), 389–405.

Lélé, I.M. and Lamb, P.J. 2010. Variability of the intertropical front (ITF) and rainfall over the west African Sudan–Sahel zone. *Journal of Climate*, 23(14), 3984–4004. ISSN 0894-8755.

Mills, G.A. and Zhao, S. 1991. A study of a monsoon depression bringing record rainfall over Australia. Part I: Numerical predictability experiments. *Monthly Weather Review*, 119(9), 2053–2073.

Nicholls, N. 2001. The insignificance of significance testing. *Bulletin of the American Meteorological Society*, 82(5), 981–986.

Pytharoulis, I. and Thorncroft, C. 1999. The low-level structure of African easterly waves in 1995. *Monthly Weather Review*, 127(10), 2266–2280.

Reed, R.J., Norquist, D.C. and Recker, E.E. 1977. The structure and properties of African wave disturbances as observed during phase III of GATE. *Monthly Weather Review*, 105(3), 317–333.

Simmons, A., Uppala, S., Dee, D. and Kobayashi, S. 2007. ERA-Interim: New ECMWF reanalysis products from 1989 onwards. *ECMWF Newsletter*, 110, 25–35.

Yang, G.Y. and Slingo, J. 2001. The diurnal cycle in the tropics. *Monthly Weather Review*, 129(4), 784–801. ISSN 0027-0644.